Available online at www.ijournalse.org

**Emerging Science Journal**

(ISSN: 2610-9182)

Vol. 7, No. 6, December, 2023

# Improving Sensitivity of the DEWMA Chart with Exact ARL Solution under the Trend AR(p) Model and Its Applications

Kotchaporn Karoon [1], Yupaporn Areepong [2*]

[1] *Department of Mathematics, Faculty of Science, Naresuan University, Phitsanulok, 65000, Thailand.*

[2] *Department of Applied Statistics, Faculty of Applied Science, King Mongkut's University of Technology North Bangkok, Bangkok 10800, Thailand.*

**Abstract**

The double exponentially weighted moving average (DEWMA) chart is a control chart that is a vital analytical tool for keeping track of the quality of a process, and the sensitivity of the control chart to the process is evaluated using the average run length (ARL). Herein, the aim of this study is to derive the explicit formula of the ARL on the DEWMA chart with the autoregressive with trend model and its residual, which is exponential white noise. This study shows that this proposed method was compared to the ARL derived using the numerical integral equation (NIE) approach, and the explicit ARL formula decreased the computing time. By changing exponential parameters that were relevant to evaluating in various circumstances, the sensitivity of AR(p) with the trend model with the DEWMA chart was investigated. These were compared with the EWMA and CUSUM charts in terms of the ARL, standard deviation run length (SDRL), and median run length (MRL). The results indicate that the DEWMA chart has the highest performance, and when it was small, the DEWMA chart had high sensitivity for detecting processes. Digital currencies are utilized to demonstrate the efficacy of the proposed method; the results are consistent with the simulated data.

**Keywords:**

Average Run Length;
DEWMA Chart;
EWMA Chart;
Autoregressive with Trend.

**Article History:**

| | | | |
|---|---|---|---|
| **Received:** | 20 | May | 2023 |
| **Revised:** | 08 | August | 2023 |
| **Accepted:** | 11 | October | 2023 |
| **Published:** | 01 | December | 2023 |

## 1- Introduction

Control charts are a type of statistical method that is useful for identifying process changes and monitoring the quality of industrial processes. They are used in a variety of industries, including finance, medicine, the environment, and others. The most basic type of memory chart is the Shewhart control chart [1], which only has sensitivity for large shifts in the process that occur. On the other hand, it is not suitable for detecting small and medium-sized changes. The memory-type charts, like the cumulative sum (CUSUM) and exponentially weighted moving average (EWMA) charts, are susceptible to spotting small and moderate changes in the process. The CUSUM chart was proposed on page [2], while Roberts introduced the traditional EWMA chart [3] for monitoring the process. Many researchers have taken these control charts and applied them in various fields. For example, Astill et al. [4] utilized the CUSUM chart to monitor financial data in the presence of time-varying volatility, such as Bitcoin.

Perry [5] used the EWMA chart for monitoring social networks and used the data to open-source Enron's email corpus. Abdallah et al. [6] utilized the EWMA chart to monitor packaging defects in the food industry. In addition, many researchers developed control charts based on the EWMA-type chart that had more sensitivity than the traditional EWMA chart for monitoring small shifts in the process. For instance, Alpaben & Jyoti [7] proposed the modified exponentially weighted moving average (MEWMA) chart, which is particularly useful for detecting small, persistent

* **CONTACT**: yupaporn.a@sci.kmutnb.ac.th

**DOI:** http://dx.doi.org/10.28991/ESJ-2023-07-06-03

shifts in the process mean or covariance matrix. In 2017, it was revised by Khan et al. [8]. Naveed et al. (2018) [9] suggested a new modified EWMA-type chart, which refers to the extended exponentially weighted moving average (EEWMA) chart and has sensitivity for monitoring small changes. Moreover, there is a control chart that outperforms in monitoring small changes rapidly. It is a double exponentially weighted moving average (DEWMA) control chart, which Shamma & Shamma first showed in 2010 [10], with modifications made by Mahmoud and Woodall [11].

Typically, a control chart must make the assumption that the data produced by the primary procedure will be independent and have a normal distribution. Nevertheless, in reality, this assumption is frequently violated because the observations or real-world data may show various patterns, and the data is mostly related to time series characteristics and forecasting. Time series and forecasting data display seasonal, trend, and autocorrelation traits. Autoregressive (AR) and moving average (MA) time series components are frequently observed when analyzing real-world data. How to assess the errors is a crucial factor to think about when creating a model. A majority of the data is normally distributed with white noise, which indicates errors in the time series model when using autocorrelated data. However, in certain situations, white noise may follow an exponential distribution [12, 13].

The ARL, which consists of two characteristics, can be used to evaluate control chart effectiveness. The in-control ARL, also known as $ARL_0$, represents the average amount of observations taken by a process under control before it signals an indication of being out-of-control. Out-of-control ARL, also known as ARL1, is the average number of observations needed to identify an alteration in a process variable that is out of control. The $ARL_0$ values should ideally be high. $ARL_1$ values, on the other hand, should ideally be as low as possible to demonstrate that the procedure is sensitive enough to rapidly identify any out-of-control situations. Calculating the ARL as a starting point is the goal when developing a control chart. In many literary works, different approaches to calculating the ARL have been proposed. For example, Champ & Rigdon [14] studied and compared the Markov Chain and the NIE method for calculating the ARL of quality control charts. Brook & Evans [15] presented the Markov Chain method for computing ARL. Karoon et al. [16] proposed the NIE method for evaluating ARL. The method cited above can be applied to a variety of data characteristics, especially real-world data, which contains many forms of autocorrelation and whose distribution does not meet the assumptions.

In addition to the methods mentioned above, there is one method of evaluating ARL, namely explicit formulas, and many researchers have studied them for various control charts. In their article, Petcharat et al. [17] explicitly established the ARL of random observations from an MA process with exponential white noise acting on the CUSUM chart. With a long-memory ARFIMA process, Sunthornwat et al. [18] assigned explicit formulations for the analytical ARL on the EWMA chart and compared them to the NIE method. An exact formula for the ARL using data from the MA(p) model was put forth by Supharakonsakun [19]. When the data are the AR(1) and AR(p) models, Karoon et al.'s explicit formula for ARL on the EEWMA chart was suggested in 2022 [20, 21]. Moreover, in the same year, they proposed exact formulas of the ARL based on the data that are autoregressive with seasonality for the EEWMA chart [22]. Areepong & Peerajit [23] used the ARL that they obtained from explicit formulas of the CUSUM chart to detect changes in the long-memory SARFIMAX model.

Phanthuna & Areepong [24] presented the explicit formula of ARL running on the MEWMA chart that shows the detection sensitivity of a modified EWMA chart under a time series model with fractionality and integration. The MEWMA chart had high performance when compared to the EWMA chart in all situations. Next, the explicit formula of the ARL underlying the data, which is seasonal autoregressive with explanatory variables on the CUSUM chart, was presented and expressed the performance of it by Phanyaem (2022) [25]. Peerajit & Areepong [26] presented the ARL of an autoregressive fractionally integrated process with exponential white noise running on the modified EWMA control chart. And also, Silpakob et al. [27] presented the explicit ARL formulas on the new MEWMA chart running on the AR(p) process. In the same year, Silpakob et al. [28] presented the explicit formula of the ARL under the ARMA with explanatory variables that is running on the MEWMA chart, and the results show that it outperformed the EWMA and CUSUM charts. Peerajit [29] said that while the process is operating on long memory under SFIMAX for the CUSUM chart, the explicit formula of ARL outperforms the ARL that is obtained using the NIE approaches. Of special interest, several researchers have also adapted analytical integral equations based on explicit formulas and the NIE technique on a control chart for models with trend variables, which are basic characteristics of the presently available data. For instance, Phanthuna et al. [30] proposed explicit formulas for the ARL that can be used to detect shifts in the MEWMA chart. These formulas are based on the trend-stationary AR(1) process.

Petcharat [31] presented the exact formulas of the ARL on the CUSUM chart running on trend with a stationary SAR process. Supharakonsakun and Areepong [32] improved the performance of the MEWMA chart by using the explicit formula of the ARL, which is processed based on the observations and is a trend autoregressive with an explanatory model. And recently, Karoon et al. [33, 34] presented the exact ARL formulas on the EEWMA chart based on the data: trend AR and quadratic trend AR models, and compared the efficiency with the EWMA chart, finding that it had more sensitivity than the EWMA chart.

All of the above-mentioned literature makes me realize that the exact formula deriving the ARL of the DEWMA chart based on the data requires an autoregressive with trend model, or trend AR(p), which has not been done before. Hence, the main objective of this paper is to use the DEWMA chart to generate specific ARL formulas for the data and compare them with the NIE method, which utilizes autoregressive with trend models. The DEWMA chart is then created using the precise ARL formula, which is enlarged to allow for a comparison of the control chart's sensitivity to the EWMA and CUSUM charts that underlie both simulated and real-world data. Then, the sensitivity of the DEWMA chart was calculated using the SDRL and MRL values, and control chart performance measures, namely the extra-square loss mean (AEQL) and comparative efficiency index (PCI), were used to confirm the results of the proposed ARL of the DEWMA chart. Moreover, the applications that were used to illustrate this research are related to digital currency, specifically referring to cryptocurrencies, namely Bitcoin and Ethereum, which are well-known among investors and are popular investments in the present. Finally, the significance of this proposed ARL is to improve the sensitivity of detecting changes in DEWMA charts using an exact ARL solution, which can be useful for the actual data generated in the autocorrelation with the trend autoregressive model to increase the efficiency of the control chart while the process changes are slight.

## 2- Structures of the Control Charts with Trend AR Model

This part includes the DEWMA statistical structure, data from the autoregressive with trend model (trend AR(p)), followed by the obtained explicit formula, and the NIE method of the ARL.

### *2-1- The EWMA Chart*

First, Robert [3] initially suggested the original idea for the EWMA chart. It is frequently used to monitor the process and identify slight deviations from the mean. The statistics of the EWMA chart can be described using the expression in Equation 1 below:

$$Z_t = \lambda Y_t + (1-\lambda)Z_{t-1}, \;\; t = 1,2,3,\ldots \tag{1}$$

where the EWMA chart parameter $Y_t$ is a sequence of autoregressive with trend or (trend AR(p)) model and a sequence data at $t = 1,2,3,\ldots$ with exponential white noise, $\lambda$ is an exponential smoothing parameter $(0,1]$, $Y_t$ at $t = 0$ is the initial value of the EWMA statistics. Its mean equals $\mu$and variance of $Y_t$equals$\frac{\lambda\sigma^2}{(2-\lambda)}$. The mean ($\mu$) and standard deviation ($\sigma$) can be used to characterize both the upper and lower control limits (UCL and LCL) and had a control width limit with $\tilde{Z}$ in Equation 2 as follows:

$$UCL = \mu + \tilde{Z}\sigma\sqrt{\frac{\lambda}{2-\lambda}}, \text{ and } LCL = \mu - \tilde{Z}\sigma\sqrt{\frac{\lambda}{2-\lambda}} \tag{2}$$

The stopping time of the EWMA chart can be specified as $\tau_{b*} = inf\{t \geq 0: Z_t > UCL\}$.

### *2-2- The DEWMA Chart*

Second, after Shamma & Shamma first suggested the DEWMA control chart in 1992 [10], Mahmoud & Woodall [11] developed it in 2010. It was explained from the EWMA control chart after being smoothed twice exponentially. The expression in Equation 3 below can be used to explain the statistics of the DEWMA control chart.

$$D_t = \lambda_2 Z_t + (1-\lambda_2)D_{t-1} \text{and} Z_t = \lambda_1 Y_t + (1-\lambda_1)\,Z_{t-1}, t = 1,2,3,\ldots \tag{3}$$

where the DEWMA chart parameter $Y_t$ is a sequence of autoregressive with trend (trend AR(p)) model and sequence data at $t = 1,2,3,\ldots$ with exponential white noise, $\lambda_1$ and $\lambda_2$ are exponential smoothing parameters equals$(0,1]$, $Y_t$ at $t = 0$ is the initial value of the DEWMA statistics. Its mean equals $\mu$and variance of $Y_t$equals$Y_t = \frac{\lambda_1^2\lambda_2^2}{(\lambda_1-\lambda_2)^2}\sigma^2\left[\frac{(1-\lambda_2)^2}{1-(1-\lambda_2)^2} + \frac{(1-\lambda_1)^2}{1-(1-\lambda_1)^2} - 2\frac{(1-\lambda_1)(1-\lambda_2)}{1-(1-\lambda_1)(1-\lambda_2)}\right]$. The mean ($\mu$) and standard deviation ($\sigma$) can be used to characterize both the upper and lower control limits (UCL and LCL), and had a control width limit with $\tilde{D}$ in Equation 4 as follows:

$$\begin{aligned} UCL &= \mu + \tilde{D}\sigma\sqrt{\frac{\lambda_1^2\lambda_2^2}{(\lambda_1-\lambda_2)^2}\left[\frac{(1-\lambda_2)^2}{1-(1-\lambda_2)^2} + \frac{(1-\lambda_1)^2}{1-(1-\lambda_1)^2} - 2\frac{(1-\lambda_1)(1-\lambda_2)}{1-(1-\lambda_1)(1-\lambda_2)}\right]}, \\ LCL &= \mu - \tilde{D}\sigma\sqrt{\frac{\lambda_1^2\lambda_2^2}{(\lambda_1-\lambda_2)^2}\left[\frac{(1-\lambda_2)^2}{1-(1-\lambda_2)^2} + \frac{(1-\lambda_1)^2}{1-(1-\lambda_1)^2} - 2\frac{(1-\lambda_1)(1-\lambda_2)}{1-(1-\lambda_1)(1-\lambda_2)}\right]}. \end{aligned} \tag{4}$$

The stopping time of the EWMA chart can be specified as: $\tau_b = inf\{t \geq 0: D_t > UCL\}$. Additionally, the DEWMA statistic becomes the EWMA statistic if $\lambda_1 = 1$.

### *2-3- The CUSUM Chart*

Third, Page (1959) designed the CUSUM chart for quality control, which can be used to spot small differences in process mean. The statistics of the CUSUM chart can be expressed using the algorithm in Equation 5 as follows:

$$C_t = max(0, C_{t-1} + Y_t - \vartheta), t = 1,2,3,\ldots \quad (5)$$

where $\vartheta$is non-zero constant, $C_0 = \Theta$ is the initial value of CUSUM; $\Theta \in [0, b']$ and the CUSUM chart's stopping time is described as $\tau_{b'} = inf\{t > 0; C_t > UCL\}$.

### *2-4- The Trend AR(p) Model of DEWMA Chart*

The two types of time-series data are steady data and non-stationary data. Gathering time-series data using stationary data does not reveal any trends or periodic effects. Non-stationary time-series data refers to time-series datasets that exhibit patterns or periodic impacts, unlike stationary time-series data that only contain random errors as a source of variance. Data points collected over time may contain internal structures (such as autocorrelation, trend, or seasonal fluctuation). Other measures, such as the moving average (MA(q)), the autoregressive moving average (ARMA(p,q)), and others, can also be used to describe a trend model. The trend AR(p) model, also known as the autoregressive with trend model, was examined in this paper. The trend autoregressive model for lag p, called trend AR (p), is written in Equation 6 as:

$$Y_t = \varpi + \gamma t + \phi_1 Y_{t-1} + \phi_2 Y_{t-2} + \ldots + \phi_p Y_{t-p} + \xi_t \quad (6)$$

where $\varpi$ is the constant of the model, $^{\gamma}$ is a slop,$\phi_i, i = 1,2,\ldots,p$ is coefficients of autoregressive $\phi_i \in [0,1]$. It is assumed that the error term $(\xi_t)$ is an exponential white noise$(\xi_t \sim Exp(\Lambda))$. The probability density function of $\xi_t$ is defined as$f(y, \Lambda) = \frac{1}{\Lambda} e^{-\frac{y}{\Lambda}}; \Lambda > 0$, and then initial values of the trend AR(p) model are $Y_{t-1}, Y_{t-2}, \ldots, Y_{t-p}$.

## 3- Methods and Measurement of Efficiency for Control Chart

For the DEWMA chart on underlying autoregressive with trend model, the initial value of ARL denoted $D(\psi)$, and the initial value of the monitoring DEWMA statistic $D_0 = \psi$ represented at $\psi \in [a, b]$. As the result, the function $D(\psi)$ is given as$ARL = D(\psi) = E_\infty(\tau_b)$. Thus,

$$ARL = D(\psi) = \begin{cases} ARL_0 = E_\infty(\tau_b), & (no \quad change), \quad in - control \quad process \\ ARL_1 = E_1(\tau_b), & (change), \quad out - of - control \quad process \end{cases}$$

where $E_\infty(\cdot)$represents the expectation with the density function as $f(y, \Lambda)$. Next, it can be used in the following section about process detecting. The change-point in model is considered as follows:

$$\xi_t \sim \begin{cases} Exp(\Lambda_0), & t = 1,2,3,\ldots,\theta - 1 \\ Exp(\Lambda_1), & t = \theta, \theta + 1, \theta + 2, \ldots \end{cases}$$

Herein, $\theta = \infty$ is the in-control ARL ($ARL_0$) and there has been no change in the statistical control process. In contrast, $\theta = 1$ denotes the first time point in the statistical control process when a change occurs from $\Lambda_0$ to$\Lambda$, which is referred to the out-of-control ARL ($ARL_1$).

### *3-1- Analytical Explicit Formulas of the ARL for Trend AR(p) Model*

This section solves the mathematically explicit formula for the ARL on the DEWMA chart using a trend autoregressive model with an exponential noise distribution. The LCL and UCL are both assumed to be equivalent to $a$and $b$, respectively. The explicit formula of the ARL is derived on the DEWMA chart with the trend AR(p) model. Let's start by substituting Equation 6 into Equation 3 as follows:

$$D_t = \lambda_1\lambda_2\left(\varpi + \gamma t + \phi_1 Y_{t-1} + \phi_2 Y_{t-2} + \ldots + \phi_p Y_{t-p} + \xi_t\right) + \lambda_2(1 - \lambda_1)Z_{t-1} + (1 - \lambda_2)D_{t-1}$$

where the first time $t = 1$ such that $D_0 = \psi$ is determined, then the initial values $Z_0 = \eta$ and $Y_{t-1}, Y_{t-2}, \ldots, Y_{t-p}$ equals 1. The following is a description of the DEWMA data with trend AR(p):

$$D_1 = \lambda_1\lambda_2\left(\varpi + \gamma t + \phi_1 Y_{t-1} + \phi_2 Y_{t-2} + \ldots + \phi_p Y_{t-p} + \xi_1\right) + \lambda_2(1 - \lambda_1)\eta + (1 - \lambda_2)\psi.$$

In control process, the interval of $D_1$ between the lower and upper bound control limits are expressed to be $a$and $b$can be written as follows below. The interval $D_1$ between the lower and upper bound control limits, can be represented as follows:

$$a < \lambda_1\lambda_2\left(\varpi + \gamma t + \phi_1 Y_{t-1} + \phi_2 Y_{t-2} + \ldots + \phi_p Y_{t-p}\right) + \lambda_2(1-\lambda_1)\eta + (1-\lambda_2)\psi + \lambda_1\lambda_2\xi_1 < b.$$

On the variable $\xi_1$, it is possible to rewrite this interval as:

$$\begin{bmatrix} \frac{a-(1-\lambda_2)\psi}{\lambda_1\lambda_2} - \frac{\lambda_2(1-\lambda_1)\eta}{\lambda_1\lambda_2} \\ -\frac{\lambda_1\lambda_2\left(\varpi+\gamma t+\phi_1 Y_{t-1}+\phi_2 Y_{t-2}+\ldots+\phi_p Y_{t-p}\right)}{\lambda_1\lambda_2} \end{bmatrix} < \xi_1 < \begin{bmatrix} \frac{b-(1-\lambda_2)\psi}{\lambda_1\lambda_2} - \frac{\lambda_2(1-\lambda_1)\eta}{\lambda_1\lambda_2} \\ -\frac{\lambda_1\lambda_2\left(\varpi+\gamma t+\phi_1 Y_{t-1}+\phi_2 Y_{t-2}+\ldots+\phi_p Y_{t-p}\right)}{\lambda_1\lambda_2} \end{bmatrix}.$$

Next, the Fredholm integral equation is used to describe the integral equation of the ARL on the DEWMA chart for the trend AR(p) model with an initial value $D_0 = \psi$. The equation rearranged is

$$D(\psi) = \int_{\left[\frac{a-(1-\lambda_2)\psi}{\lambda_1\lambda_2} - \frac{\lambda_2(1-\lambda_1)\eta}{\lambda_1\lambda_2} - \frac{\lambda_1\lambda_2\left(\omega+\gamma+\phi_1 Y_{t-1}+\phi_2 Y_{t-2}+\ldots+\phi_p Y_{t-p}\right)}{\lambda_1\lambda_2}\right]}^{\left[\frac{b-(1-\lambda_2)\psi}{\lambda_1\lambda_2} - \frac{\lambda_2(1-\lambda_1)\eta}{\lambda_1\lambda_2} - \frac{\lambda_1\lambda_2\left(\varpi+\gamma+\phi_1 Y_{t-1}+\phi_2 Y_{t-2}+\ldots+\phi_p Y_{t-p}\right)}{\lambda_1\lambda_2}\right]} D(\upsilon)\cdot f(\upsilon)d\upsilon,$$

$$\upsilon = \lambda_1\lambda_2\left(\varpi + \gamma + \phi_1 Y_{t-1} + \phi_2 Y_{t-2} + \ldots + \phi_p Y_{t-p}\right) + (1-\lambda_2)\psi + \lambda_2(1-\lambda_1)\eta + \lambda_1\lambda_2\xi_1 .$$

Let $D(\psi)$ denote the *ARL* on the DEWMA chart for the trend AR(p) model. We use the second kind of Fredholm integral equation to solve the ARL [35]. The formula is displayed in Equation 7 as follows:

$$D(\psi) = 1 + \frac{1}{\lambda_1\lambda_2}\int_a^b D(\upsilon) f\left(\frac{\upsilon-(1-\lambda_2)\psi-\lambda_2(1-\lambda_1)\eta-\lambda_1\lambda_2\left(\varpi+\gamma+\phi_1 Y_{t-1}+\phi_2 Y_{t-2}+\ldots+\phi_p Y_{t-p}\right)}{\lambda_1\lambda_2}\right) d\upsilon \tag{7}$$

Eventually, the function $D(\psi)$ expresses the error terms, or the function $\xi_1$, as an exponential distribution function. Hence, the following is a description of the function $D(\psi)$ in Equation 8:

$$D(\psi) = 1 + \frac{1}{\Lambda\lambda_1\lambda_2}\cdot e^{\frac{(1-\lambda_2)\psi}{\Lambda\lambda_1\lambda_2}}\cdot e^{\frac{\lambda_2(1-\lambda_1)\eta}{\Lambda\lambda_1\lambda_2}}\cdot e^{\frac{\lambda_1\lambda_2\left(\varpi+\gamma+\phi_1 Y_{t-1}+\phi_2 Y_{t-2}+\ldots+\phi_p Y_{t-p}\right)}{\Lambda}}\int_a^b D(\upsilon)\cdot e^{\frac{-\upsilon}{\Lambda\lambda_1\lambda_2}} d\upsilon. \tag{8}$$

The fixed-point theorem of Banach is used to confirm the ARL solution. In terms of its existence and uniqueness, this is characterized as an ARL solution [36]. From Equation 8, suppose that

$$G(\psi) = \frac{1}{\Lambda\lambda_1\lambda_2}\cdot e^{\frac{(1-\lambda_2)\psi}{\Lambda\lambda_1\lambda_2}}\cdot e^{\frac{\lambda_2(1-\lambda_1)\eta}{\Lambda\lambda_1\lambda_2}}\cdot e^{\frac{\lambda_1\lambda_2\left(\varpi+\gamma+\phi_1 Y_{t-1}+\phi_2 Y_{t-2}+\ldots+\phi_p Y_{t-p}\right)}{\Lambda}} \text{ and } \Phi = \int_a^b L(\upsilon)\cdot e^{\frac{-\upsilon}{\beta\lambda_1\lambda_2}} d\upsilon.$$

Therefore, the ARL solution that is obtained by Equation 8 can be rewritten that showed in Equation 9 as follows:

$$D(\psi) = 1 + G(\psi)\cdot\Phi \tag{9}$$

Later, the integral equation $\Phi$, which can be expressed as:

$$\Phi = \int_a^b e^{\frac{-\upsilon}{\Lambda\lambda_1\lambda_2}}\cdot\left(1 + \frac{1}{\Lambda\lambda_1\lambda_2}\cdot e^{\frac{(1-\lambda_2)\psi}{\Lambda\lambda_1\lambda_2}}\cdot e^{\frac{\lambda_2(1-\lambda_1)\eta}{\Lambda\lambda_1\lambda_2}}\cdot e^{\frac{\lambda_1\lambda_2\left(\varpi+\gamma+\phi_1 Y_{t-1}+\phi_2 Y_{t-2}+\ldots+\phi_p Y_{t-p}\right)}{\Lambda}}\cdot\Phi\right) d\upsilon$$

$$\Phi = \frac{-\Lambda\lambda_1\lambda_2\left[e^{\frac{-b}{\Lambda\lambda_1\lambda_2}} - e^{\frac{-a}{\Lambda\lambda_1\lambda_2}}\right]}{1+\frac{1}{\lambda_2}\cdot e^{\frac{1}{\Lambda}\cdot\left(\varpi+\gamma+\phi_1 Y_{t-1}+\phi_2 Y_{t-2}+\ldots+\phi_p Y_{t-p}\right)+\frac{1}{\Lambda\lambda_1}\cdot(1-\lambda_1)\eta}\cdot\left[e^{\frac{-b}{\Lambda\lambda_1}} - e^{\frac{-a}{\Lambda\lambda_1}}\right]} \tag{10}$$

Finally, Equation 10, which is replaced in Equation 9, is substituted into the solution of $\Phi$, and the following result is obtained in Equation 11 as:

$$D(\psi) = 1 - \frac{\lambda_2 e^{\frac{(1-\lambda_2)\psi}{\Lambda\lambda_1\lambda_2}}\cdot\left[e^{\frac{-b}{\Lambda\lambda_1\lambda_2}} - e^{\frac{-a}{\Lambda\lambda_1\lambda_2}}\right]}{\lambda_2 e^{\frac{1}{\Lambda}\cdot\left(\varpi+\gamma+\phi_1 Y_{t-1}+\phi_2 Y_{t-2}+\ldots+\phi_p Y_{t-p}\right)+\frac{1}{\Lambda\lambda_1}\cdot(1-\lambda_1)\eta} + \left[e^{\frac{-b}{\Lambda\lambda_1}} - e^{\frac{-a}{\Lambda\lambda_1}}\right]}. \tag{11}$$

As the trend AR(p) model is applied to the DEWMA chart, Equation 11 provides the explicit ARL formula. Moreover, $\Lambda_0$ is used to replace the in-control process, while$\Lambda_1$; $\Lambda_1 = (1+\delta)\Lambda_0$ is used to replace the out-of-control process. And also, $\delta$ stands for the shift size in the monitoring process.

### 3-2- Analytical NIE of the ARL for Trend AR(p) Model

This section solves the analytical NIE approach for the ARL on the DEWMA chart using a trend autoregressive model with an exponential noise distribution. Let $\widehat{D}(\psi)$ represent the midpoint quadrature rule-computed ARL of the DEWMA chart for the trend AR(p) model with an exponential white noise. In particular, we computed in terms of the $m$ linear equation systems with the midpoint rule on the interval $[a, b]$, and this method was split into $a \le s_1 \le s_2 \le \ldots \le s_m \le b$ using a set of constant weights $w_j = (b-a)/m$ after using a quadrature rule. The approximation for an integral can be determined by applying the quadrature rule, which is represented in Equation 12 below

$$\int_a^b D(v)f(v)dv \approx \sum_{j=1}^{m} w_j f(s_j) \tag{12}$$

The NIE approach; $\widehat{D}(s_i)$, which is evaluated by a linear equation, had shown in Eq. (13), as follows

$$\widehat{D}(s_i) = 1 + \frac{1}{\lambda_1\lambda_2}\sum_{j=1}^{m} \widehat{D}(s_j) \cdot f\left(\frac{s_j-(1-\lambda_2)s_i-\lambda_1\lambda_2(\varpi+\gamma+\phi_1 Y_{t-1}+\phi_2 Y_{t-2}+\ldots+\phi_p Y_{t-p})-\lambda_2(1-\lambda_1)\eta}{\lambda_1\lambda_2}\right) \tag{13}$$

Finally, $s_i$is instead of $\psi$ into $\widehat{D}(s_i)$, the NIE approximating of the ARL is rewritten in Equation 14 as follows

$$\widehat{D}(\psi) \approx 1 + \frac{1}{\lambda_1\lambda_2}\sum_{j=1}^{m} \widehat{D}(\psi_j) \cdot f\left(\frac{s_j-(1-\lambda_2)\psi-\lambda_1\lambda_2(\varpi+\gamma+\phi_1 Y_{t-1}+\phi_2 Y_{t-2}+\ldots+\phi_p Y_{t-p})-\lambda_2(1-\lambda_1)\eta}{\lambda_1\lambda_2}\right) \tag{14}$$

where $s_j$is the division point within the interval $a \le s_1 \le s_2 \le \ldots \le s_m \le b$ as well as$s_j = (j-0.5)w_j + a$ for $j = 1,2,\ldots,m$. And then, a weight of the composite midpoint formula is given as $w_j = (b-a)/m$

### 3-3- The Existence and Uniqueness of Exact ARL Solution

In this part, this study also uses Banach's fixed-point theorem to prove the ARL solution's existence and uniqueness because the explicit ARL formula must prove its existence and uniqueness. Let $T$represent the operation in the class of all continuous functions, which is expressed as:

$$T(D(\psi)) = 1 + \frac{1}{\lambda_1\lambda_2}\int_a^b D(v) f\left(\frac{v-(1-\lambda_2)\psi-\lambda_2(1-\lambda_1)\eta-\lambda_1\lambda_2(\varpi+\gamma+\phi_1 Y_{t-1}+\phi_2 Y_{t-2}+\ldots+\phi_p Y_{t-p})}{\lambda_1\lambda_2}\right) dv$$

Theorem 1 Banach's Fixed-point Theorem: Let $(Y, D)$ and $T: Y \to Y$represent a complete metric space and the contraction mapping, respectively. And then, $T$ is referred to unique on fixed point. There exists a unique solution to the fixed point when $T(D(\psi)) = D(\psi) \in Y$.

To proof that, let $T$ determined in Eq. (7) represent the contraction mapping for $D(\psi)_1, D(\psi)_2 \in \psi[a, b]$. Such that, $\|T(D(\psi)_1) - T(D(\psi)_2)\| \le \Omega\|D(\psi)_1 - (D(\psi)_2\|, D(\psi)_1, D(\psi)_2 \in Y$, where $\Omega$ is a positive constant.

By considering: $\|T(D(\psi)_1) - T(D(\psi)_2)\|_\infty = \sup_{\psi\in[a,b]} |(D(\psi)_1 - (D(\psi)_2|$

$$= \sup_{\psi\in[a,b]} \left| \frac{1}{\Lambda\lambda_1\lambda_2} \cdot e^{\frac{(1-\lambda_2)\psi}{\Lambda\lambda_1\lambda_2}} \cdot e^{\frac{\lambda_2(1-\lambda_1)\eta}{\Lambda\lambda_1\lambda_2}} \cdot e^{\frac{\lambda_1\lambda_2(\varpi+\gamma+\phi_1 Y_{t-1}+\phi_2 Y_{t-2}+\ldots+\phi_p Y_{t-p})}{\Lambda}} \int_a^b (D_1(v) - D_2(v)) \cdot e^{\frac{-v}{\Lambda\lambda_1\lambda_2}} dv \right|$$

$$\le \sup_{\psi\in[a,b]} \left| \|D(\psi)_1 - D(\psi)_2\|_\infty \cdot e^{\frac{(1-\lambda_2)\psi}{\Lambda\lambda_1\lambda_2}} \cdot e^{\frac{\lambda_2(1-\lambda_1)\eta}{\Lambda\lambda_1\lambda_2}} \cdot e^{\frac{\lambda_1\lambda_2(\varpi+\gamma+\phi_1 Y_{t-1}+\phi_2 Y_{t-2}+\ldots+\phi_p Y_{t-p})}{\Lambda}} \cdot (-\Lambda\lambda_1\lambda_2)\left(e^{\frac{-b}{\Lambda\lambda_1\lambda_2}} - e^{\frac{-a}{\Lambda\lambda_1\lambda_2}}\right) \right|$$

$$= \|D(\psi)_1 - D(\psi)_2\|_\infty \sup_{\psi\in[a,b]} \left| e^{\frac{(1-\lambda_2)\psi}{\Lambda\lambda_1\lambda_2}} \cdot e^{\frac{\lambda_2(1-\lambda_1)\eta}{\Lambda\lambda_1\lambda_2}} \cdot e^{\frac{\lambda_1\lambda_2(\varpi+\gamma+\phi_1 Y_{t-1}+\phi_2 Y_{t-2}+\ldots+\phi_p Y_{t-p})}{\Lambda}} \right| \left| e^{\frac{-a}{\Lambda\lambda_1\lambda_2}} - e^{\frac{-b}{\Lambda\lambda_1\lambda_2}} \right|$$

$$\le \Omega\|D(\psi)_1 - D(\psi)_2\|_\infty$$

where $\Omega = \sup_{\psi\in[a,b]} \left| e^{\frac{(1-\lambda_2)\psi}{\Lambda\lambda_1\lambda_2}} \cdot e^{\frac{\lambda_2(1-\lambda_1)\eta}{\Lambda\lambda_1\lambda_2}} \cdot e^{\frac{\lambda_1\lambda_2(\varpi+\gamma+\phi_1 Y_{t-1}+\phi_2 Y_{t-2}+\ldots+\phi_p Y_{t-p})}{\Lambda}} \right| \left| e^{\frac{-a}{\Lambda\lambda_1\lambda_2}} - e^{\frac{-b}{\Lambda\lambda_1\lambda_2}} \right|$ $\Omega \in [0,1)$

### 3-4- The Measurement of Efficiency for the Control Chart

The average run length (ARL) is a popular measurement used to assess the performance of control charts. The ARL, produced by explicit equations, and the NIE method, which uses an autoregressive with trend process, or trend AR process, to detect changes, were employed to compare their findings on the DEWMA chart. The percentage accuracy (%Acc) indicates the relative efficiency of two methods of the ARL, which is given in Equation 15 as follows:

$$\%Acc = 100 - \left(\left|\frac{D(\psi)-\widehat{D}(\psi)}{D(\psi)}\right| \times 100\%\right) \tag{15}$$

Next, the efficiency of the ARL is calculated with different parameter values based on the DEWMA chart. It is then used for comparison with the EWMA and CUSUM charts. In addition, some other characteristics of the run length (RL)

exist, namely the standard deviation run length (SDRL) and the median run length (MRL). Those are additional metrics for the evaluation of control charts. The equations in Equation 16 are used to determine SDRL and MRL for in-control [26]:

$$ARL_0 = \frac{1}{\alpha}, SDRL_0 = \sqrt{\frac{1-\alpha}{\alpha^2}}, MRL_0 = \frac{log(0.5)}{log(1-\alpha)}, \quad (16)$$

where type I error represents $\alpha = 1 - P(a < Y_t < b|\Lambda_0)$. In this study, $ARL_0$ was fixed at 370. Form an $ARL_0$ value that can be calculated as $SDRL_0$ and $MRL_0$ by Equation 16 at approximately 370 and 256, respectively. On the other hand, SDRL and MRL are calculated by the formulas in Equation 17 for out-of-control situations. The values obtained by those formulas are the lowest; the result indicates that control charts provide the best performance [26]

$$ARL_1 = \frac{1}{1-\beta}, SDRL_1 = \sqrt{\frac{\beta}{(1-\beta)^2}}, MRL_1 = \frac{log(0.5)}{log\,\beta}, \quad (17)$$

where type II error represents $\beta = 1 - P(a < Y_t < b|\Lambda_1)$. Moreover, when shift sizes differ, using the ARL measurement to assess how well control charts affect the process is reasonable. Many studies recommend using overall performance metrics to evaluate a control chart's success during different changes ($\delta max_{min}$). Some of them feature performance measurements, including the average extra quadratic loss (AEQL) and the performance comparison index (PCI), that are used to evaluate their effectiveness [37].

The mathematical formula for the AEQL is:

$$AEQL = \frac{1}{\Delta}\sum_{\delta=\delta_{min}}^{\delta_{max}\Sigma}\left(\delta^2 \times 1 - \frac{\lambda_2 e^{\frac{(1-\lambda_2)\psi}{\Lambda\lambda_1\lambda_2}}\cdot\left[e^{\frac{-b}{\Lambda\lambda_1\lambda_2}} - e^{\frac{-a}{\Lambda\lambda_1\lambda_2}}\right]}{\lambda_2 e^{\frac{1}{\Lambda}\left(\varpi+\gamma+\phi_1 Y_{t-1}+\phi_2 Y_{t-2}+\ldots+\phi_p Y_{t-p}\right)+\frac{1}{\Lambda\lambda_1}(1-\lambda_1)\eta}+\left[e^{\frac{-b}{\Lambda\lambda_1}} - e^{\frac{-a}{\Lambda\lambda_1}}\right]}\right) \quad (18)$$

where $\delta$ is the particular change in the process, and Δ is the sum of number of divisions from $\delta_{min}$to $\delta_{max}$. In this study, $\Delta = 7$ is determined from $\delta_{min}$ to $\delta_{max}$. The control charts with the lowest AEQL values perform the best.

The PCI measurement is the ratio between the AEQLs of the control chart and the most efficient control chart, which is shown as the lowest AEQL. The mathematical formula for the PCI is

$$PCI = \frac{AEQL}{AEQL_{lowest}} \quad (19)$$

The PCI value of the most efficient control chart is 1, while the less efficient control chart will give a PCI value greater than 1.

### *3-5- The Procedure of Analytical Results of the ARL*

he ARL for spotting changes in the process is a standard metric for evaluating a control chart's effectiveness. The effectiveness of the explicit formula and the NIE approach for calculating the ARL for monitoring shifts were evaluated in this study. The DEWMA chart running on the trend AR models, specifically the trend AR(1), trend AR(2), and trend AR(3), was used to evaluate the performance with exponential white noise. The residual of an exponential distribution with uncorrelated data is what is known as "exponential white noise," as was previously mentioned. As a consequence, $\delta = 0$ represents an in-control process, while $\delta > 0$ represents an out-of-control process. The NIE approach is used to determine the number of division points, m = 500, using the ARL approximation. The NIE approach is used to determine the number of division points, $m$ = 500, using the ARL approximation. The explicit ARL and the NIE approach to the ARL were computed using the Mathematica program. Through research, the Intel(R) Xeon(R) CPU X5680 @ 3.33 GHz (3 processors) RAM 32.0 GB specification for Mathematica was evaluated. The following is a brief description of the procedure:

***Step 1:*** Give the input parameters, such as the coefficients of autoregressive ($\phi_i$), the initial values of the autoregressive; $Y_{t-1}, Y_{t-2}, \ldots, Y_{t-p}$, and the control chart parameters set as $\lambda_1 = 0.05, 0.10, \lambda_2 = 0.05$.

***Step 2:*** Determine the initial value of known parameter ($\varpi$), slope value of the trend AR(p) model ($\gamma$) and the initial value of the DEWMA statistic ($Z_0 = \eta$ and$D_0 = \psi$).

***Step 3:*** Impose the parameter of exponential white noise; $\Lambda = \Lambda_0$ for the in-control process.

***Step 4:*** Specify the lower control limit;$a = 0$ and fixed the ARL value of in-control equals 370 to compute the upper control limit ($b$).

***Step 5:*** Define the upper control limit ($b$) from Step 4. Compute the ARL values of out-of-control by the explicit formula and the NIE method, determine parameter of exponential white noise ($\Lambda = \Lambda_1$) where $\Lambda_1 = \Lambda_0(1 + \delta)$, and change shift sizes ($\delta$) equals 0.001, 0.002, 0.01, 0.02, 0.1, 0.5, and 1, respectively.

Also, solutions can be found using the approach depicted in Figure 1.

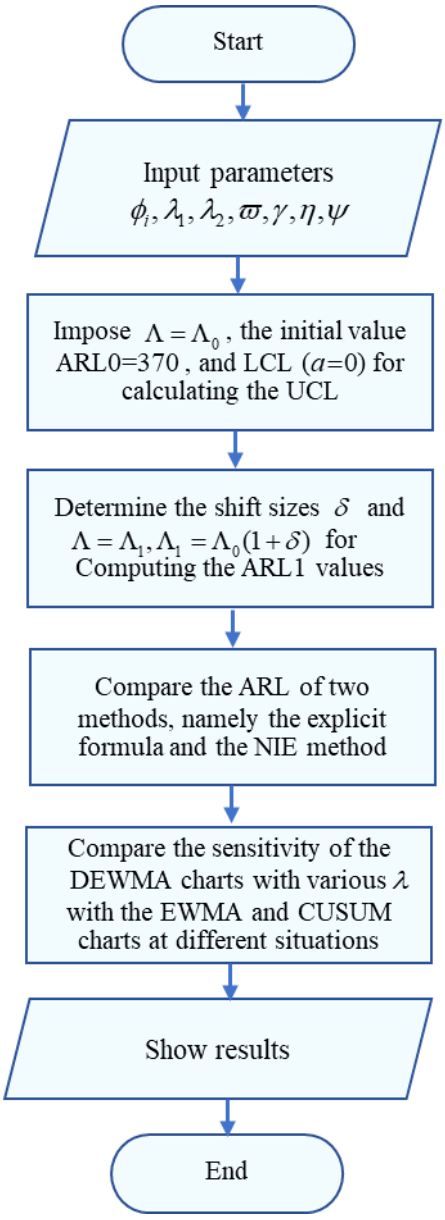


**Figure 1. The process of methodology diagram**

## 4- Results and Discussions

### *4-1- The Simulated Results*

For the in-control scenario, the simulated data is frequently given with $ARL_0$ = 370, allowing the beginning parameters to be explored at $\Lambda_0 = 1$. On the other hand, $\Lambda_1 = \Lambda_0(1+\delta)$ is researched in the out-of-control scenario and computed to determine shift sizes. At the interval [0, $b$], the lower and higher control limits are investigated. First, the ARL was evaluated using the explicit formula and the NIE method, and the capability of the methods was compared with the %Acc. The results were computed based on specified known parameters, such as $\phi_1 = 0.1, \phi_2 = 0.2, \phi_3 = 0.3, \varpi = 0$, and $\gamma = 0.5$ . There are three models, namely the trend AR(1), trend AR(2), and trend AR(3) models, that were determined with exponentially smoothing parameters as follows in Table 1. The explicit formula technique's ARL values, represented as $D(\psi)$, are calculated using Equation 11. The $\widehat{D}(\psi)$ is then indicated using the NIE approach and is computed using Equation 14. All circumstances have a very high percentage of acceptance, about 100. However, the explicit formula appears very instantly in all circumstances, but the ARL values obtained using the NIE approach take roughly 3–4 seconds to compute. As a result, it makes sense to proceed with these precise formulations. The comparative results of accuracy and computational speed on the DEWMA chart are consistent with the research of Areepong & Peerajit (2022) [23], which obtained an explicit formula for ARL in the CUSUM chart. Then it's consistent with the research of Karoon et al. [33], which offers an explicit ARL solution for detecting changes on EEWMA with Trend's AR(p) process and validating the proposal with ARL's NIE method. Obviously, it takes almost no computation time compared to the NIE method.

**Table 1. The ARL values of the explicit formula against the NIE method for trend AR(p) models on the DEWMA chart with known parameters, $\lambda_2 = 0.05, \phi_1 = 0.1, \phi_2 = 0.2, \phi_3 = 0.3, \varpi = 0$, and $\gamma = 0.5$ under different conditions**

| $\delta$ | Model | Trend AR(1) | | Trend AR(2) | | Trend AR(3) | |
|---|---|---|---|---|---|---|---|
| | $\lambda_1$ | 0.05 | 0.10 | 0.05 | 0.10 | 0.05 | 0.10 |
| | $b$ | 0.0000306203 | 0.000453442 | 0.0000250683 | 0.000371087 | 0.0000185698 | 0.000274769 |
| 0.000 | $D(\psi)$ | 370.232 (<0.01) | 370.158 (<0.01) | 370.130 (<0.01) | 370.257 (<0.01) | 370.240 (<0.01) | 370.151 (<0.01) |
| | $\widehat{D}(\psi)$ | 370.232 (3.858) | 370.158 (3.875) | 370.130 (4.079) | 370.257 (4.157) | 370.240 (4.031) | 370.151 (4.14) |
| | %Acc | 100.00 | 100.00 | 100.00 | 100.00 | 100.00 | 100.00 |
| 0.001 | $D(\psi)$ | 123.491 (<0.01) | 160.569 (<0.01) | 120.598 (<0.01) | 156.097 (<0.01) | 116.514 (<0.01) | 149.702 (<0.01) |
| | $\widehat{D}(\psi)$ | 123.491 (3.859) | 160.569 (3.937) | 120.598 (4.093) | 156.097 (4.078) | 116.514 (4.157) | 149.702 (4.078) |
| | %Acc | 100.00 | 100.00 | 100.00 | 100.00 | 100.00 | 100.00 |
| 0.002 | $D(\psi)$ | 74.320 (<0.01) | 102.723 (<0.01) | 72.251 (<0.01) | 99.100 (<0.01) | 69.354 (<0.01) | 94.030 (<0.01) |
| | $\widehat{D}(\psi)$ | 74.320 (3.781) | 102.723 (3.875) | 72.251 (4.077) | 99.100 (3.984) | 69.354 (4.297) | 94.030 (4.297) |
| | %Acc | 100.00 | 100.00 | 100.00 | 100.00 | 100.00 | 100.00 |
| 0.01 | $D(\psi)$ | 18.199 (<0.01) | 26.943 (<0.01) | 17.613 (<0.01) | 25.749 (<0.01) | 16.801 (<0.01) | 24.123 (<0.01) |
| | $\widehat{D}(\psi)$ | 18.199 (3.813) | 26.943 (3.844) | 17.613 (4.031) | 25.749 (4.110) | 16.801 (4.094) | 24.123 (4.219) |
| | %Acc | 100.00 | 100.00 | 100.00 | 100.00 | 100.00 | 100.00 |
| 0.02 | $D(\psi)$ | 9.654 (<0.01) | 14.342 (<0.01) | 9.345 (<0.01) | 13.694 (<0.01) | 8.916 (<0.01) | 12.816 (<0.01) |
| | $\widehat{D}(\psi)$ | 9.654 (3.953) | 14.342 (3.983) | 9.345 (4.141) | 13.694 (4.062) | 8.916 (4.281) | 12.816 (4.172) |
| | %Acc | 100.00 | 100.00 | 100.00 | 100.00 | 100.00 | 100.00 |
| 0.1 | $D(\psi)$ | 2.541 (<0.01) | 3.589 (<0.01) | 2.474 (<0.01) | 3.442 (<0.01) | 2.381 (<0.01) | 3.243 (<0.01) |
| | $\widehat{D}(\psi)$ | 2.541 (4.047) | 3.589 (3.859) | 2.474 (4.063) | 3.442 (4.000) | 2.381 (4.171) | 3.243 (4.188) |
| | %Acc | 100.00 | 100.00 | 100.00 | 100.00 | 100.00 | 100.00 |
| 0.5 | $D(\psi)$ | 1.180 (<0.01) | 1.415 (<0.01) | 1.167 (<0.01) | 1.379 (<0.01) | 1.149 (<0.01) | 1.333 (<0.01) |
| | $\widehat{D}(\psi)$ | 1.180 (3.937) | 1.415 (3.890) | 1.167 (4.094) | 1.379 (4.031) | 1.149 (4.156) | 1.333 (4.203) |
| | %Acc | 100.00 | 100.00 | 100.00 | 100.00 | 100.00 | 100.00 |
| 1 | $D(\psi)$ | 1.058 (<0.01) | 1.173 (<0.01) | 1.053 (<0.01) | 1.155 (<0.01) | 1.045 (<0.01) | 1.131 (<0.01) |
| | $\widehat{D}(\psi)$ | 1.058 (3.937) | 1.173 (3.860) | 1.053 (4.062) | 1.155 (4.109) | 1.045 (4.219) | 1.131 (4.110) |
| | %Acc | 100.00 | 100.00 | 100.00 | 100.00 | 100.00 | 100.00 |

Next, the capability of the explicit ARL based on the DEWMA chart running on the trend AR(p) model is compared with the EWMA and CUSUM charts and then investigated using different $\lambda$. For out-of-control, the results for contrasting capability between the DEWMA, EWMA, and CUSUM charts based on different situations are shown in Tables 2 and 3. The results showed that the DEWMA chart obtained lower $ARL_1$, $SDRL_1$, and $MRL_1$ values than the EWMA and CUSUM charts in all situations for both the trend AR(1) and trend AR(2) models, whereas the RL results based on shift sizes that are defined as $\delta \geq 0.1$show that the results of the EWMA chart are very close to the results of the DEWMA chart. In addition, the AEQL and PCI values are also utilized to validate their efficacy. The $ARL_1$ values of all charts were used for calculating the AEQL and PCI values, which were computed from Equations 18 and 19, respectively. The results show that the AEQL values of the DEWMA chart are lower than the AEQL values of the EWMA and CUSUM charts, and the PCI values of the DEWMA chart with $\lambda_1 = 0.05$ are equal to 1, just as they are for the trend AR(1) and trend AR(2) models. From the research results mentioned above, the performance of DEWMA shows superior performance in detecting transition changes compared to EWMA and CUSUM charts, and the smaller the exponential smoothing parameter, the greater the capabilities of the DEWMA chart. The findings are consistent with previously presented studies showing that the explicit formula of the ARL generalized modified EWMA-type was more effective than the original EWMA; see [21, 24].

**Table 2. The $ARL_1$ values of the explicit formula for trend AR(1) model on the DEWMA, EWMA, and CUSUM charts with known parameters, $\lambda_2 = 0.05, \varpi = 0$, and $\gamma = 0.5$ under different conditions**

| $\phi_i$ | | $\phi_1 = 0.3$ | | | | $\phi_1 = -0.3$ | | | |
|---|---|---|---|---|---|---|---|---|---|
| $\delta$ | Control chart | DEWMA1 ($\lambda_1 = 0.05$) | DEWMA2 ($\lambda_1 = 0.10$) | EWMA ($\lambda_1 = 1$) | CUSUM ($\vartheta = 3$) | DEWMA1 ($\lambda_1 = 0.05$) | DEWMA2 ($\lambda_1 = 0.10$) | EWMA ($\lambda_1 = 1$) | CUSUM ($\vartheta = 3$) |
| | UCL | 0.0000250683 | 0.000371087 | 0.0226722 | 4.145 | 0.0000456873 | 0.000677249 | 0.0417181 | 3.265 |
| 0.001 | $ARL_1$ | 116.514 | 149.702 | 194.952 | 367.173 | 129.632 | 170.154 | 227.528 | 367.902 |
| | $SDRL_1$ | 116.013 | 149.201 | 194.451 | 366.673 | 129.131 | 169.653 | 227.027 | 367.402 |
| | $MRL_1$ | 80.414 | 103.419 | 134.784 | 254.158 | 89.507 | 117.595 | 157.364 | 254.664 |

| | | | | | | | | | |
|---|---|---|---|---|---|---|---|---|---|
| | $ARL_1$ | 69.354 | 94.030 | 132.526 | 364.365 | 78.792 | 110.663 | 164.447 | 365.599 |
| 0.002 | $SDRL_1$ | 68.852 | 93.528 | 132.025 | 363.865 | 78.290 | 110.162 | 163.946 | 365.099 |
| | $MRL_1$ | 47.725 | 64.829 | 91.513 | 252.212 | 54.267 | 76.359 | 113.639 | 253.067 |
| | $ARL_1$ | 16.801 | 24.123 | 37.759 | 342.859 | 19.490 | 29.642 | 51.739 | 347.839 |
| 0.01 | $SDRL_1$ | 16.293 | 23.617 | 37.256 | 342.359 | 18.984 | 29.138 | 51.236 | 347.339 |
| | $MRL_1$ | 11.295 | 16.371 | 25.825 | 237.305 | 13.160 | 20.198 | 35.515 | 240.757 |
| | $ARL_1$ | 8.916 | 12.816 | 20.319 | 318.200 | 10.339 | 15.815 | 28.322 | 327.203 |
| 0.02 | $SDRL_1$ | 8.401 | 12.306 | 19.812 | 317.700 | 9.826 | 15.307 | 27.818 | 326.703 |
| | $MRL_1$ | 5.827 | 8.532 | 13.734 | 220.213 | 6.814 | 10.612 | 19.283 | 226.453 |
| | $ARL_1$ | 2.381 | 3.243 | 4.992 | 184.532 | 2.691 | 3.928 | 6.944 | 208.758 |
| 0.1 | $SDRL_1$ | 1.813 | 2.697 | 4.465 | 184.031 | 2.134 | 3.392 | 6.424 | 208.257 |
| | $MRL_1$ | 1.272 | 1.880 | 3.101 | 127.561 | 1.492 | 2.359 | 4.457 | 144.353 |
| | $ARL_1$ | 1.149 | 1.333 | 1.775 | 32.563 | 1.211 | 1.498 | 2.306 | 45.642 |
| 0.5 | $SDRL_1$ | 0.414 | 0.666 | 1.173 | 32.059 | 0.506 | 0.863 | 1.736 | 45.139 |
| | $MRL_1$ | 0.339 | 0.500 | 0.836 | 22.222 | 0.397 | 0.629 | 1.219 | 31.288 |
| | $ARL_1$ | 1.045 | 1.131 | 1.376 | 12.151 | 1.072 | 1.218 | 1.693 | 16.513 |
| 1 | $SDRL_1$ | 0.217 | 0.385 | 0.719 | 11.640 | 0.278 | 0.515 | 1.084 | 16.005 |
| | $MRL_1$ | 0.220 | 0.321 | 0.534 | 8.071 | 0.257 | 0.403 | 0.776 | 11.096 |
| AEQL | | 0.196 | 0.220 | 0.255 | 4.289 | 0.201 | 0.235 | 0.255 | 4.311 |
| PCI | | 1.000 | 1.122 | 1.299 | 21.839 | 1.000 | 1.166 | 1.268 | 21.428 |

**Table 3. The $ARL_1$ values of the explicit formula for trend AR(2) model on the DEWMA, EWMA, and CUSUM charts with known parameters, $\lambda_2 = 0.05, \varpi = 0$, and $\gamma = 0.5$ under different conditions.**

| $\phi_i$ | | $\phi_1 = \phi_2 = 0.3$ | | | | $\phi_1 = 0.3, \phi_2 = -0.3$ | | | |
|---|---|---|---|---|---|---|---|---|---|
| $\delta$ | Control chart | **DEWMA1 ($\lambda_1 = 0.05$)** | **DEWMA2 ($\lambda_1 = 0.10$)** | **EWMA ($\lambda_1 = 1$)** | **CUSUM ($\vartheta = 3$)** | **DEWMA1 ($\lambda_1 = 0.05$)** | **DEWMA2 ($\lambda_1 = 0.10$)** | **EWMA ($\lambda_1 = 1$)** | **CUSUM ($\vartheta = 3$)** |
| | UCL | **0.0000185698** | **0.000274769** | **0.01674441** | **4.887** | **0.0000338418** | **0.0005012559** | **0.03073175** | **3.663** |
| | $ARL_1$ | 115.255 | 147.657 | 191.934 | 366.813 | 124.976 | 162.858 | 215.152 | 367.658 |
| 0.001 | $SDRL_1$ | 114.754 | 147.156 | 191.433 | 366.313 | 124.475 | 162.357 | 214.651 | 367.158 |
| | $MRL_1$ | 79.542 | 102.001 | 132.692 | 253.909 | 86.280 | 112.538 | 148.785 | 254.494 |
| | $ARL_1$ | 68.452 | 92.434 | 129.761 | 363.590 | 75.393 | 104.608 | 151.851 | 365.285 |
| 0.002 | $SDRL_1$ | 67.951 | 91.933 | 129.260 | 363.090 | 74.891 | 104.107 | 151.350 | 364.785 |
| | $MRL_1$ | 47.100 | 63.723 | 89.596 | 251.675 | 51.911 | 72.162 | 104.908 | 252.850 |
| | $ARL_1$ | 16.547 | 23.620 | 36.674 | 339.028 | 18.506 | 27.576 | 45.884 | 347.003 |
| 0.01 | $SDRL_1$ | 16.039 | 23.115 | 36.170 | 338.528 | 17.999 | 27.072 | 45.382 | 346.503 |
| | $MRL_1$ | 11.119 | 16.023 | 25.072 | 234.650 | 12.478 | 18.766 | 31.457 | 240.177 |
| | $ARL_1$ | 8.782 | 12.546 | 19.710 | 311.144 | 9.817 | 14.687 | 24.935 | 325.800 |
| 0.02 | $SDRL_1$ | 8.267 | 12.036 | 19.203 | 310.644 | 9.303 | 14.178 | 24.429 | 325.300 |
| | $MRL_1$ | 5.734 | 8.345 | 13.312 | 215.322 | 6.452 | 9.829 | 16.934 | 225.481 |
| | $ARL_1$ | 2.352 | 3.182 | 4.846 | 166.402 | 2.577 | 3.668 | 6.114 | 205.069 |
| 0.1 | $SDRL_1$ | 1.783 | 2.635 | 4.318 | 165.901 | 2.016 | 3.129 | 5.592 | 204.568 |
| | $MRL_1$ | 1.252 | 1.837 | 2.999 | 114.994 | 1.411 | 2.178 | 3.881 | 141.796 |
| | $ARL_1$ | 1.143 | 1.319 | 1.736 | 25.057 | 1.188 | 1.434 | 2.081 | 43.288 |
| 0.5 | $SDRL_1$ | 0.405 | 0.649 | 1.130 | 24.552 | 0.472 | 0.788 | 1.500 | 42.785 |
| | $MRL_1$ | 0.334 | 0.488 | 0.807 | 17.019 | 0.376 | 0.580 | 1.058 | 29.657 |
| | $ARL_1$ | 1.043 | 1.124 | 1.353 | 10.225 | 1.061 | 1.183 | 1.558 | 15.600 |
| 1 | $SDRL_1$ | 0.211 | 0.373 | 0.691 | 9.713 | 0.255 | 0.466 | 0.933 | 15.092 |
| | $MRL_1$ | 0.217 | 0.314 | 0.516 | 6.735 | 0.243 | 0.372 | 0.675 | 10.463 |
| AEQL | | 0.195 | 0.215 | 0.244 | 3.186 | 0.199 | 0.227 | 0.244 | 4.091 |
| PCI | | 1.000 | 1.105 | 1.253 | 16.378 | 1.000 | 1.142 | 1.227 | 20.598 |

### *4-2- The Real-World Datasets*

Two applications, the prices of Bitcoin and Ethereum, are brought up for analysis in this section, utilizing daily datasets and the trend AR(1) and trend AR(2) models, respectively. Those were fitted as the models by SPSS. The results for two datasets that are suitable inputs for the trend AR(p) model and display suitable parameters are shown in Table 4. The significance of white noise's fit to the exponential mean was then determined using the one-sample Kolmogorov-Smirnov test, as shown in Table 5.

**Table 4. The coefficients for the trend AR(p) models using the real-world datasets**

| Application | Application 1: Trend AR(1) model | | | | Application 2: Trend AR(2) model | | | |
|---|---|---|---|---|---|---|---|---|
| parameters | Coefficient | Std. Error | t-Statistic | p-value | Coefficient | Std. Error | t-Statistic | p-value |
| constant | 16.946 | 1.416 | 11.967 | 0 | 11.009 | 0.770 | 14.297 | 0.000 |
| trend | 0.085 | 0.038 | 24.949 | 0 | 0.066 | 0.015 | 4.416 | 0.000 |
| AR(1) | 0.948 | 0.029 | 2.931 | 0.004 | 0.685 | 0.113 | 6.053 | 0.000 |
| AR(2) | | | | | 0.242 | 0.113 | 2.130 | 0.036 |

**Table 5. One-sample Kolmogorov test for the real-world datasets**

| Residual of Application | Residual of Application 1: Trend AR(1) model | Residual of Application 2: Trend AR(2) model |
|---|---|---|
| Exponential parameter | 0.4357 | 0.2815 |
| One-sample Kolmogorov-Smirnov test | 0.540 | 0.787 |
| p-value | 0.932 | 0.566 |

For application 1, daily data of the prices of Bitcoin (unit: 1,000 USD) from December 16, 2022, to March 5, 2023. It was fitted to the trend AR(1), which expressed itself as $Y_t = 16.946 + 0.085t + 0.948Y_{t-1} + \xi_t$, where $\xi_t \sim Exp(\Lambda_0 = 0.4357)$.

For application 2, daily data of the prices of Ethereum (unit: 100 USD) from November 21, 2022 to February 8, 2023. It was fitted to the trend AR(2), which expressed itself as

$Y_t = 11.009 + 0.066t + 0.685Y_{t-1} + 0.242Y_{t-2} + \xi_t$, where $\xi_t \sim Exp(\Lambda_0 = 0.2815)$.

The $ARL_1$ values for the DEWMA (different $\lambda_1$; 0.05, 0.10), EWMA ($\lambda_1$= 1), and CUSUM charts are displayed in Table 6. According to the findings of the control chart comparison, the DEWMA chart with the lower $\lambda_1$ had a lower $ARL_1$ and performed better than the EWMA chart in every scenario. In addition, to verify performance, the AEQL and PCI values were also used in the same way as the simulated results above. The results show that the AEQL value of the DEWMA chart is lower than the AEQL values of the EWMA and CUSUM charts, and the PCI value of the DEWMA chart has $\lambda_1$ equal to 1, as in the simulated data above. As a result, the results indicate that the outcomes of two applications with underlying trend AR(1) and AR(2) models are similar to simulated data, as illustrated in Figure 2. And then, the AEQL and PCI values supported the control chart's effectiveness by using $ARL_1$ values in the formulas mentioned above. The outcomes demonstrate that, as shown in Figure 3, the DEWMA chart with $\lambda_1$ equal to 0.05 outperformed the DEWMA chart with greater $\lambda_1$ , the EWMA and CUSUM charts, all of which had higher AEQL and PCI > 1, by having the lowest AEQL and PCI equal to 1.

**Table 6. The $ARL_1$ values of the explicit formula on the DEWMA, EWMA, and CUSUM charts with real-world datasets in cases of digital currency prices with known parameters for $ARL_0$ =370**

| | | Application 1 | | | | Application 2 | | | |
|---|---|---|---|---|---|---|---|---|---|
| $\delta$ | Control chart | DEWMA1 ($\lambda_1 = 0.05$) | DEWMA2 ($\lambda_1 = 0.10$) | EWMA ($\lambda_1 = 1$) | CUSUM ($\vartheta = 3$) | DEWMA1 ($\lambda_1 = 0.05$) | DEWMA2 ($\lambda_1 = 0.10$) | EWMA ($\lambda_1 = 1$) | CUSUM ($\vartheta = 1$) |
| | UCL | 0.000000064363 | 0.0000126847 | 0.00797175 | 0.018 | 0.00000005458 | 0.0000225125 | 0.0286805 | 0.482 |
| 0.001 | $ARL_1$ | 80.203 | 120.237 | 205.480 | 368.409 | 72.757 | 122.286 | 296.067 | 367.805 |
| | $SDRL_1$ | 79.702 | 119.736 | 204.979 | 367.909 | 72.255 | 121.785 | 295.567 | 367.305 |
| | $MRL_1$ | 55.245 | 82.995 | 142.081 | 255.015 | 50.084 | 84.415 | 204.871 | 254.596 |
| 0.002 | $ARL_1$ | 40.776 | 65.430 | 132.290 | 365.924 | 40.573 | 73.459 | 246.649 | 365.482 |
| | $SDRL_1$ | 40.273 | 64.928 | 131.789 | 365.424 | 40.070 | 72.957 | 246.148 | 364.982 |
| | $MRL_1$ | 27.916 | 45.005 | 91.349 | 253.292 | 27.775 | 50.571 | 170.617 | 252.986 |
| 0.01 | $ARL_1$ | 9.595 | 16.049 | 38.430 | 349.144 | 9.962 | 19.135 | 111.122 | 349.035 |
| | $SDRL_1$ | 9.081 | 15.541 | 37.927 | 348.644 | 9.448 | 18.628 | 110.621 | 348.535 |
| | $MRL_1$ | 6.297 | 10.774 | 26.290 | 241.661 | 6.552 | 12.913 | 76.677 | 241.586 |

| | | | | | | | | | |
|---|---|---|---|---|---|---|---|---|---|
| | $ARL_1$ | 5.212 | 8.609 | 20.913 | 329.912 | 5.349 | 10.150 | 65.595 | 329.503 |
| 0.02 | $SDRL_1$ | 4.685 | 8.094 | 20.407 | 329.412 | 4.823 | 9.637 | 65.093 | 329.003 |
| | $MRL_1$ | 3.254 | 5.614 | 14.146 | 228.331 | 3.349 | 6.683 | 45.120 | 228.047 |
| | $ARL_1$ | 1.597 | 2.311 | 5.125 | 216.283 | 1.621 | 2.636 | 15.752 | 215.012 |
| 0.1 | $SDRL_1$ | 0.977 | 1.740 | 4.598 | 215.782 | 1.003 | 2.076 | 15.244 | 214.511 |
| | $MRL_1$ | 0.705 | 1.222 | 3.194 | 149.569 | 0.722 | 1.453 | 10.568 | 148.688 |
| | $ARL_1$ | 1.027 | 1.136 | 1.811 | 51.561 | 1.029 | 1.200 | 4.069 | 50.544 |
| 0.5 | $SDRL_1$ | 0.165 | 0.393 | 1.212 | 51.059 | 0.173 | 0.490 | 3.534 | 50.041 |
| | $MRL_1$ | 0.190 | 0.326 | 0.863 | 35.392 | 0.195 | 0.387 | 2.458 | 34.687 |
| | $ARL_1$ | 1.004 | 1.040 | 1.397 | 19.246 | 1.004 | 1.067 | 2.600 | 18.706 |
| 1 | $SDRL_1$ | 0.062 | 0.203 | 0.745 | 18.739 | 0.067 | 0.268 | 2.040 | 18.199 |
| | $MRL_1$ | 0.125 | 0.212 | 0.551 | 12.991 | 0.128 | 0.251 | 1.428 | 12.616 |
| AEQL | | 0.183 | 0.193 | 0.273 | 4.924 | 0.183 | 0.200 | 0.545 | 4.809 |
| PCI | | 1.000 | 1.056 | 1.496 | 26.933 | 1.000 | 1.093 | 2.976 | 26.271 |

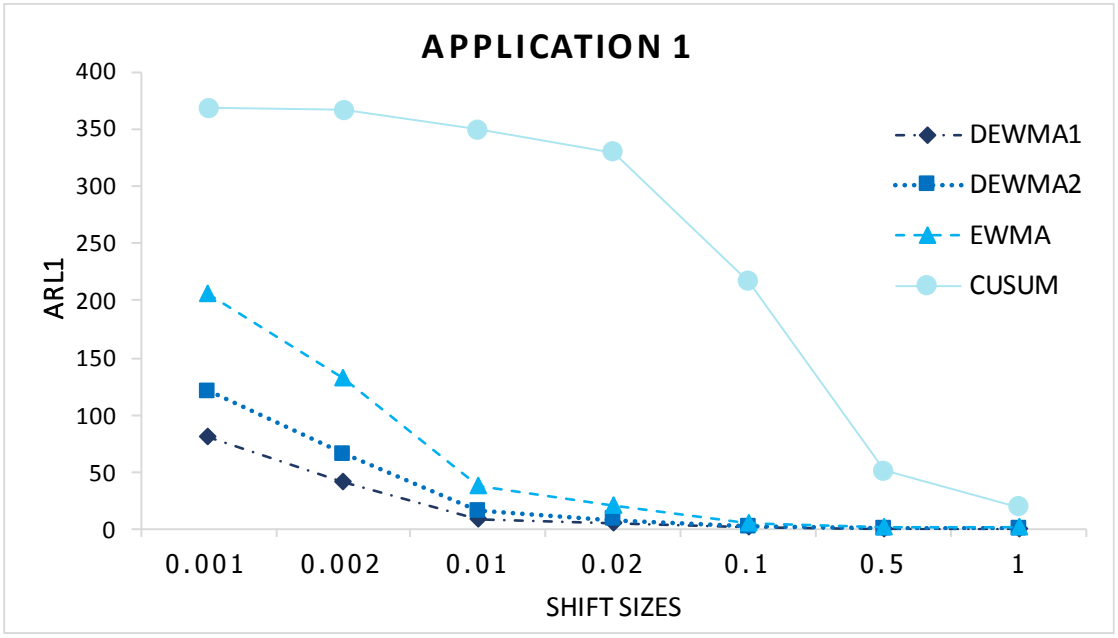


(a)

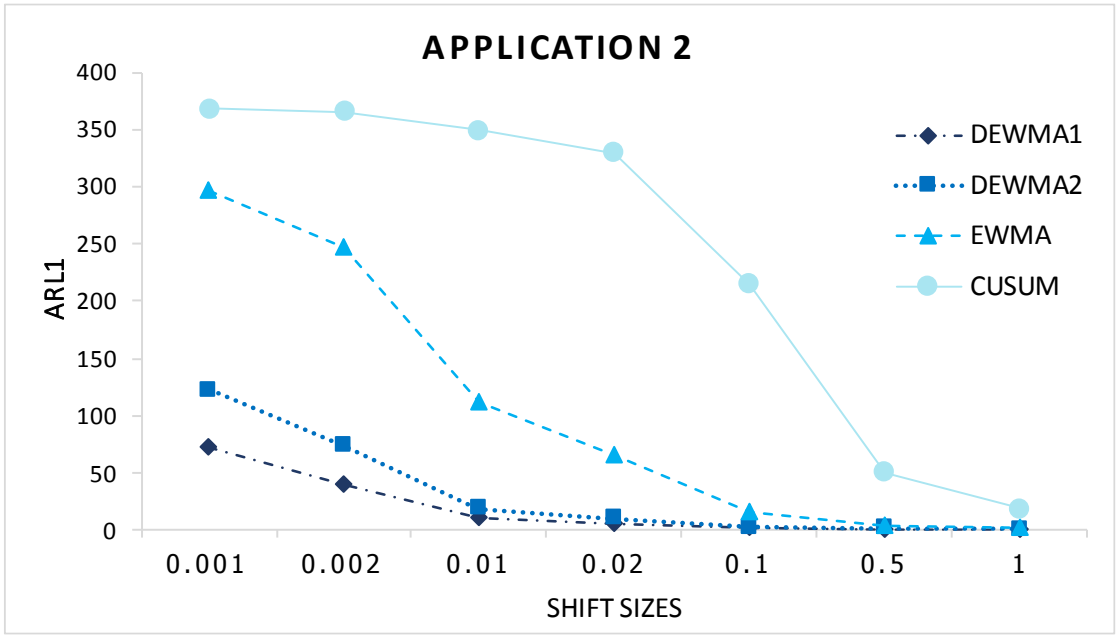


(b)

**Figure 2. $ARL_1$ values on the control charts with real-world datasets for; (a) Trend AR(1) and (b) Trend AR(2)**

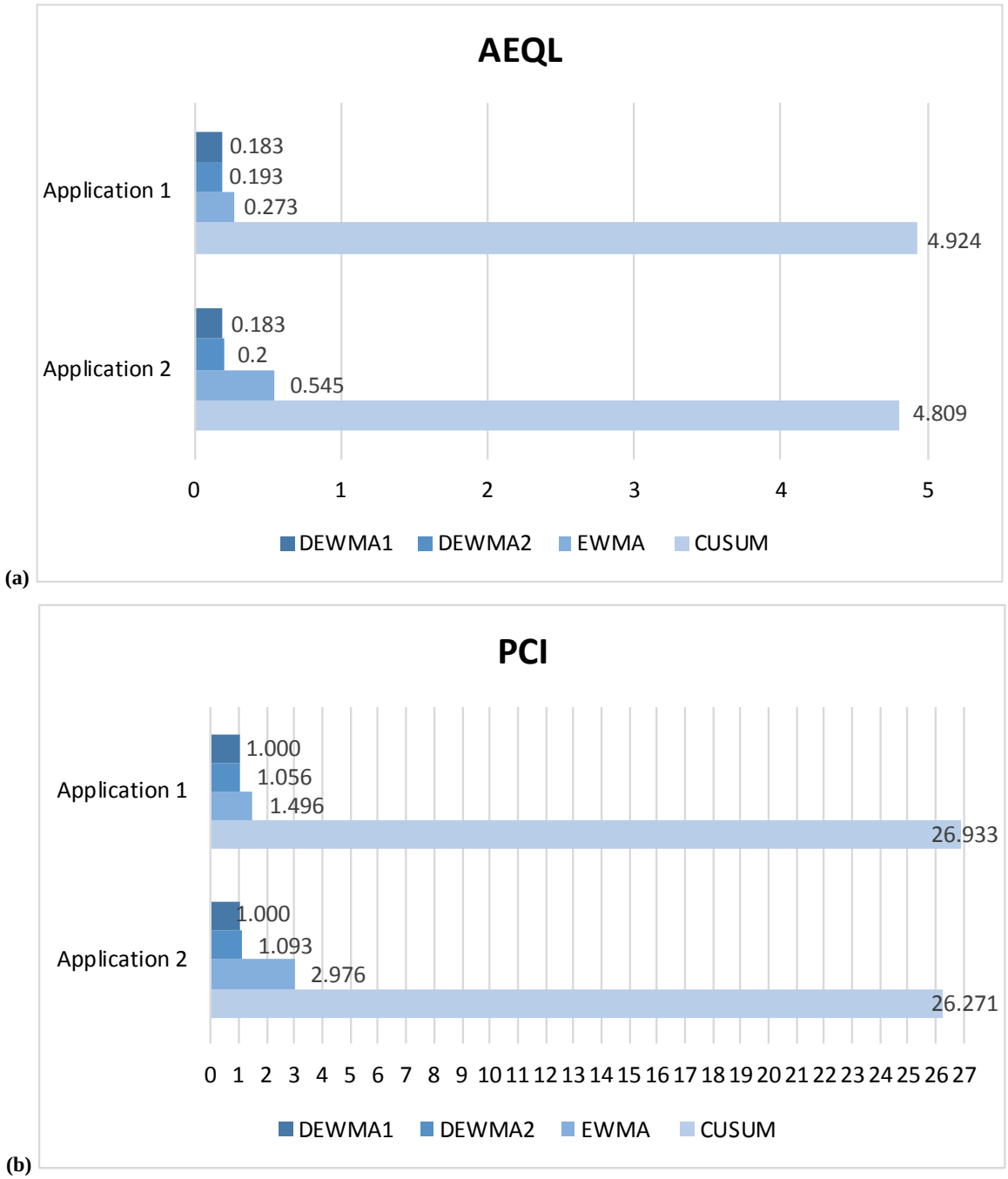


**Figure 3. AEQL and PCI values on the control charts with real-world datasets for: (a) Trend AR(1) and (b) Trend AR(2)**

After that, Figure 4 further demonstrates how well the control chart functions to identify shift changes during the monitoring process. And also, the performance of the CUSUM chart shown above indicates that CUSUM charts are significantly less effective than EWMA types such as DEWMA and EWMA charts. The CUSUM chart is therefore not shown in the detection diagram section of Figure 4. In this part, the DEWMA with $\lambda_1$ and $\lambda_2$ equals 0.10 and 0.05, that was compared to EWMA chart. While the DEWMA chart for Application 1 acknowledges shifts as being out of control at the 8$^{th}$ observation, the EWMA chart does so at the 14$^{th}$ observation. While, the DEWMA chart for Application 2 acknowledges shifts as being out of control at the 12$^{th}$ observation, but the EWMA chart does so at the 27$^{th}$ observation. According to the findings, the double EWMA control chart may be able to identify shift changes more quickly than the EWMA control chart throughout the monitoring process. Therefore, an excellent option for spotting change is the DEWMA chart, which performs the best under the situations in this study. However, this finding was shown in cases where the data were only underlying a trend autoregressive process. If the data are from another process that is not a trend autoregressive model, it may not be appropriate to use this proposed ARL on the DEWMA chart for monitoring the process mean changes and may need to be studied further.

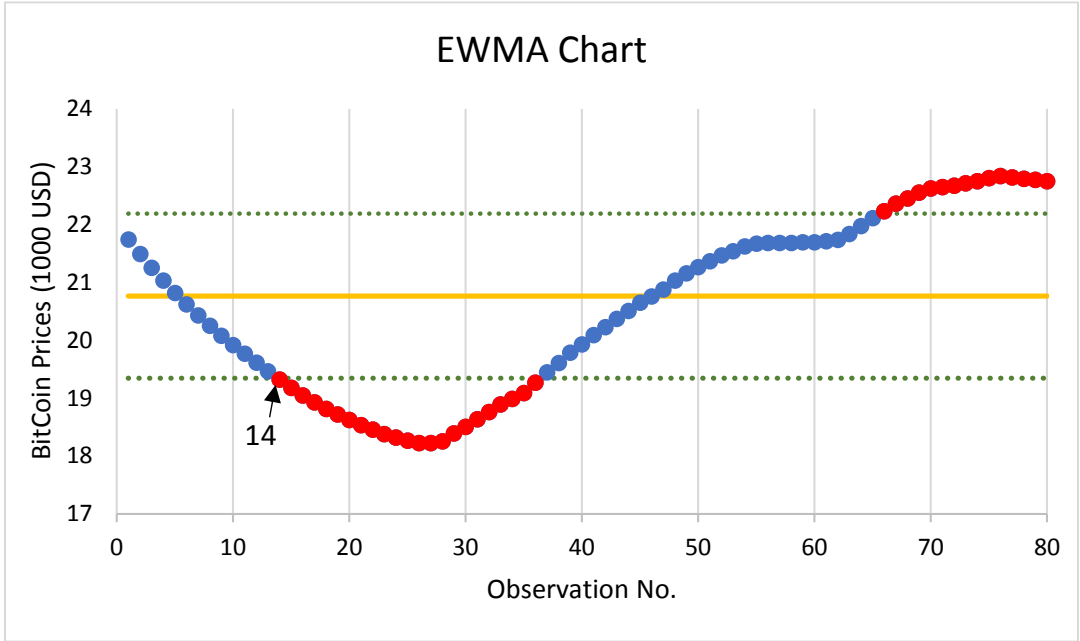
EWMA Chart
BitCoin Prices (1000 USD)
Observation No.
14
24
23
22
21
20
19
18
17
0
10
20
30
40
50
60
70
80

(a)

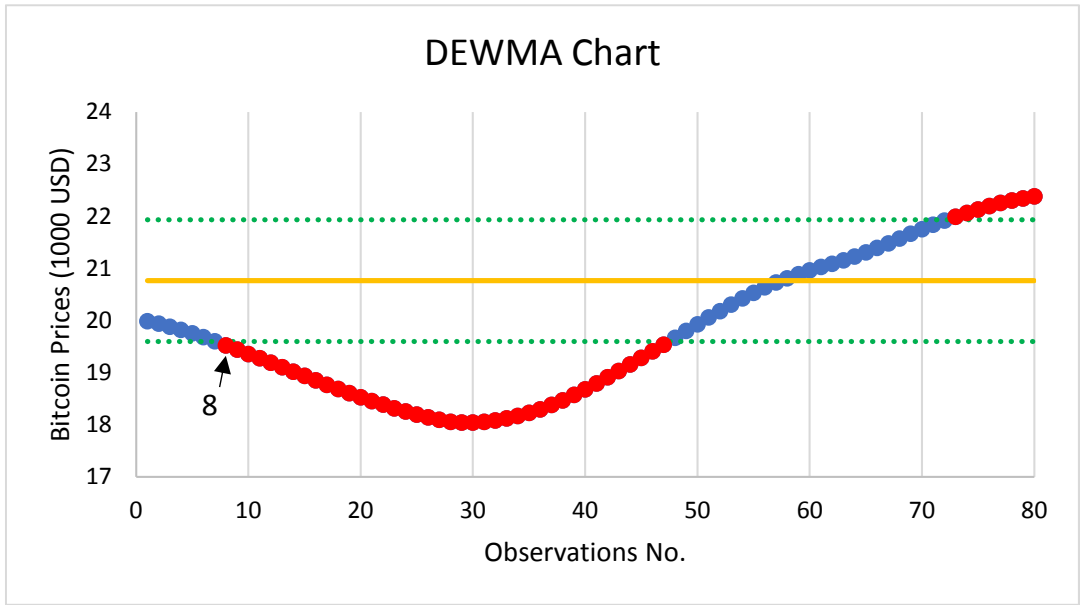
DEWMA Chart
Bitcoin Prices (1000 USD)
Observations No.
8
24
23
22
21
20
19
18
17
0
10
20
30
40
50
60
70
80

(b)

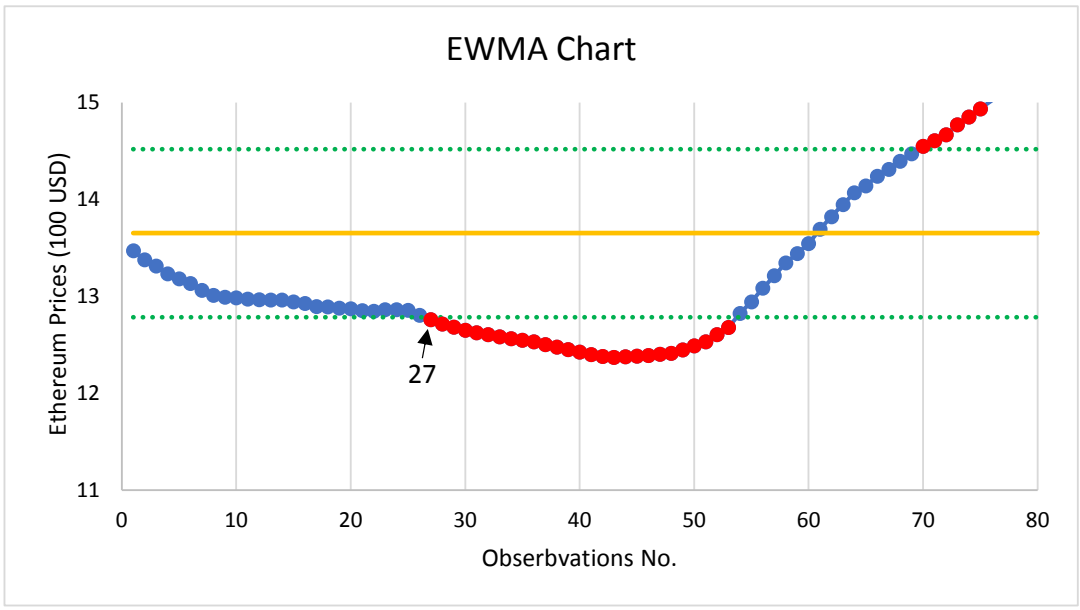
EWMA Chart
Ethereum Prices (100 USD)
Obserbvations No.
27
15
14
13
12
11
0
10
20
30
40
50
60
70
80

(c)

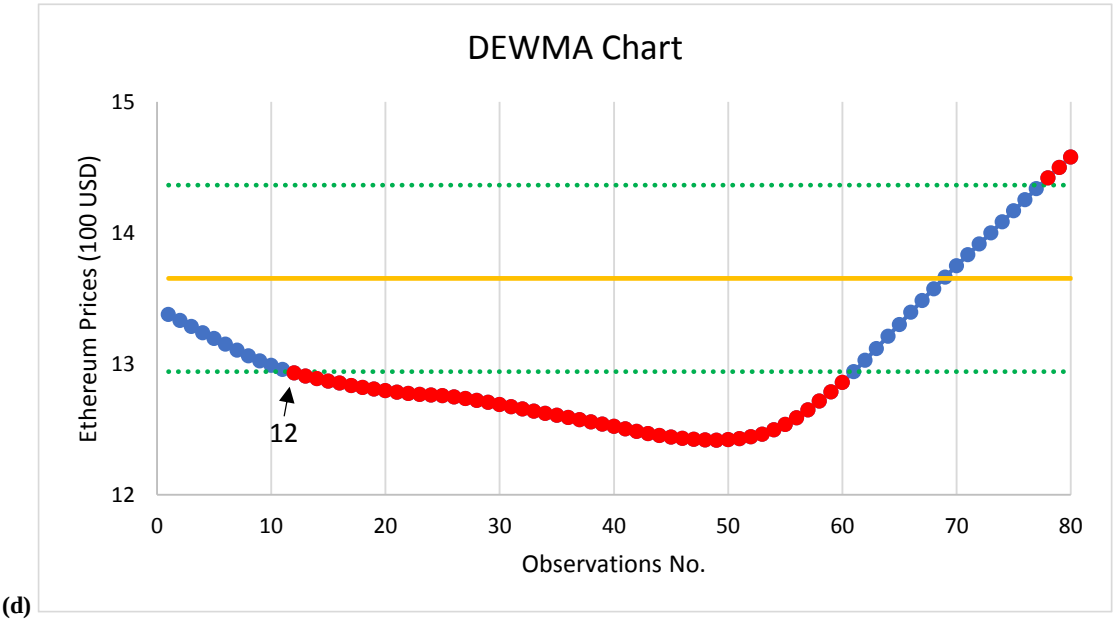


**(d)**

**Figure 4. The capability of detecting processes of control charts in cases of two applications with underlying trend AR(p) model; trend AR(1) on (a) EWMA chart, (b) DEWMA chart, and trend AR(2) on (c) EWMA chart, (d) DEWMA chart**

## 5- Conclusion

The exact ARL solution, compared in performance to the NIE approach's ARL, was found to help reduce processing time and was used to assess the sensitivity of DEWMA charts based on the running trend AR(p) model with exponential white noise. After that, the explicit ARL on running the DEWMA chart was compared to the EWMA and CUSUM charts under the out-of-control process with different shift sizes (compared by using ARL1, SDRL1, and MRL1 values). Next, the sensitivity of control charts is verified by two measures, such as AEQL and PCI. According to the results, the DEWMA chart has the highest performance, and when $\lambda$ was small, the DEWMA chart had high sensitivity for detecting processes. Additionally, actual data can be used to apply the exact ARL solutions, producing results that are identical to those of simulated data. Real-world data following the AR(p) trend model with exponential distribution white noise might be analyzed using these formulas, as might the prices of digital currencies such as Bitcoin and Ethereum, both of which were used. As a result, the explicit formula was a good method for determining the ARL for shift changes based on observations in the DEWMA chart to use a precise ARL solution, which improved the sensitivity of the DEWMA chart for parameter shift detection. In this study, the proposed explicit formula may have some limitations. It works very well only for data that is characterized as being autocorrelated with an autoregressive model. However, this research is a good starting point to further improve the sensitivity of detecting small process changes under various data formats in future scenarios. Last, future studies will be conducted on the explicit ARL formulas on the DEWMA chart to appropriate them with the other model of real data. Also, we will derive the explicit formula on modern control charts using this approach to improve their efficacy for detecting change in different situations.

## 6- Declarations

### *6-1- Author Contributions*

Conceptualization, K.K. and Y.A.; methodology, K.K.; software, K.K.; validation, K.K. and Y.A.; formal analysis, K.K.; investigation, Y.A.; resources, K.K.; data curation, Y.A.; writing—original draft preparation, K.K.; writing—review and editing, K.K.; visualization, Y.A.; supervision, Y.A.; project administration, K.K.; funding acquisition, Y.A. All authors have read and agreed to the published version of the manuscript.

### *6-2- Data Availability Statement*

Publicly available datasets were analyzed in this study. These datasets to be Bitcoin and Ethereum prices can be found here: *https://coinmarketcap.com*.

### *6-3- Funding*

This research was funded by Thailand Science Research and Innovation Fund (NSRF), and King Mongkut's University of Technology North Bangkok with Contract no. KMUTNB-FF-66-04.

### *6-4- Acknowledgements*

The authors are grateful to the referees for their constructive comments and suggestions which helped to improve this research.

### *6-5- Institutional Review Board Statement*

Not applicable.

### *6-6- Informed Consent Statement*

Not applicable.

### *6-7- Conflicts of Interest*

The authors declare that there is no conflict of interest regarding the publication of this manuscript. In addition, the ethical issues, including plagiarism, informed consent, misconduct, data fabrication and/or falsification, double publication and/or submission, and redundancies have been completely observed by the authors.

## 7- References

[1] Shewhart, W. A. (1930). Economic Quality Control of Manufactured Product1. Bell System Technical Journal, 9(2), 364–389. doi:10.1002/j.1538-7305.1930.tb00373.x.

[2] Page, E. S. (1954). Continuous Inspection Schemes. Biometrika, 41(1/2), 100. doi:10.2307/2333009.

[3] Roberts, S. W. (1959). Control Chart Tests Based on Geometric Moving Averages. Technometrics, 1(3), 239. doi:10.2307/1266443.

[4] Astill, S., Harvey, D. I., Leybourne, S. J., Taylor, A. M. R., & Zu, Y. (2023). CUSUM-Based Monitoring for Explosive Episodes in Financial Data in the Presence of Time-Varying Volatility. Journal of Financial Econometrics, 21(1), 187–227. doi:10.1093/jjfinec/nbab009.

[5] Perry, M. B. (2020). An EWMA control chart for categorical processes with applications to social network monitoring. Journal of Quality Technology, 52(2), 182–197. doi:10.1080/00224065.2019.1571343.

[6] Abdallaha, R. A., Haridy, S., Shamsuzzaman, M., & Bashir, H. (2021). An Application of EWMA Control Chart for Monitoring Packaging Defects in Food Industry. Proceedings of the International Conference on Industrial Engineering and Operations Management, Singapore, Singapore. doi:10.46254/an11.20210410.

[7] Alpaben, K. P., & Jyoti, D. (2011). Modified exponentially weighted moving average (EWMA) control chart for an analytical process data. Journal of Chemical Engineering and Materials Science, 2(1), 12–20. doi:10.5897/JCEMS.9000014.

[8] Khan, N., Aslam, M., & Jun, C. H. (2017). Design of a Control Chart Using a Modified EWMA Statistic. Quality and Reliability Engineering International, 33(5), 1095–1104. doi:10.1002/qre.2102.

[9] Naveed, M., Azam, M., Khan, N., & Aslam, M. (2018). Design of a Control Chart Using Extended EWMA Statistic. Technologies, 6(4), 108. doi:10.3390/technologies6040108.

[10] Shamma, S. E., & Shamma, A. K. (1992). Development and Evaluation of Control Charts Using Double Exponentially Weighted Moving Averages. International Journal of Quality & Reliability Management, 9(6), 18–25. doi:10.1108/02656719210018570.

[11] Mahmoud, M. A., & Woodall, W. H. (2010). An Evaluation of the double exponentially weighted moving average control chart. Communications in Statistics: Simulation and Computation, 39(5), 933–949. doi:10.1080/03610911003663907.

[12] Jacobs, P. A., & Lewis, P. A. W. (1977). A mixed autoregressive-moving average exponential sequence and point process (EARMA 1,1). Advances in Applied Probability, 9(1), 87–104. doi:10.2307/1425818.

[13] Ibazizen, M., & Fellag, H. (2003). Bayesian estimation of an AR(1) process with exponential white noise. Statistics, 37(5), 365–372. doi:10.1080/0233188031000078042.

[14] Champ, C. W., & Rigdon, S. E. (1991). A comparison of the markov chain and the integral equation approaches for evaluating the run length distribution of quality control charts. Communications in Statistics - Simulation and Computation, 20(1), 191–204. doi:10.1080/03610919108812948.

[15] Brook, D., & Evans, D. A. (1972). An approach to the probability distribution of cusum run length. Biometrika, 59(3), 539–549. doi:10.1093/biomet/59.3.539.

[16] Karoon, K., Areepong, Y., & Sukparungsee, S. (2021). Numerical integral equation methods of average run length on extended EWMA control chart for autoregressive process. Proceedings of the World Congress on Engineering (WCE 2021), 7-9 July, 2021, London, United Kingdom.

[17] Petcharat, K., Sukparungsee, S., & Areepong, Y. (2015). Exact solution of the average run length for the cumulative sum chart for a moving average process of order q. ScienceAsia, 41(2), 141–147. doi:10.2306/scienceasia1513-1874.2015.41.141.

[18] Sunthornwat, R., Areepong, Y., & Sukparungsee, S. (2017). Average run length of the long-memory autoregressive fractionally integrated moving average process of the exponential weighted moving average control chart. Cogent Mathematics, 4(1), 1358536. doi:10.1080/23311835.2017.1358536.

[19] Supharakonsakun, Y. (2021). Statistical design for monitoring process mean of a modified EWMA control chart based on autocorrelated data. Walailak Journal of Science and Technology, 18(12), 19813. doi:10.48048/wjst.2021.19813.

[20] Karoon, K., Areepong, Y., & Sukparungsee, S. (2022). Exact solution of average run length on extended EWMA control chart for the first-order autoregressive process. Thailand Statistician, 20(2), 395-411.

[21] Karoon, K., Areepong, Y., & Sukparungsee, S. (2022). Exact Run Length Evaluation on Extended EWMA Control Chart for Autoregressive Process. Intelligent Automation and Soft Computing, 33(2), 743–759. doi:10.32604/iasc.2022.023322.

[22] Karoon, K., Areepong, Y., & Sukparungsee, S. (2022). Exact run length evaluation on extended EWMA control chart for seasonal autoregressive process. Engineering Letters, 30(4), 1-14.

[23] Areepong, Y., & Peerajit, W. (2022). Integral equation solutions for the average run length for monitoring shifts in the mean of a generalized seasonal ARFIMAX(P, D, Q, r)s process running on a CUSUM control chart. PLoS ONE, 17(2), 264283. doi:10.1371/journal.pone.0264283.

[24] Phanthuna, P., & Areepong, Y. (2022). Detection Sensitivity of a Modified EWMA Control Chart with a Time Series Model with Fractionality and Integration. Emerging Science Journal, 6(5), 1134–1152. doi:10.28991/ESJ-2022-06-05-015.

[25] Phanyaem, S. (2022). Explicit Formulas and Numerical Integral Equation of ARL for SARX(P,r)L Model Based on CUSUM Chart. Mathematics and Statistics, 10(1), 88–99. doi:10.13189/ms.2022.100107.

[26] Peerajit, W., & Areepong, Y. (2023). Alternative to Detecting Changes in the Mean of an Autoregressive Fractionally Integrated Process with Exponential White Noise Running on the Modified EWMA Control Chart. Processes, 11(2), 503. doi:10.3390/pr11020503.

[27] Silpakob, K., Areepong, Y., Sukparungsee, S., & Sunthornwat, R. (2023). A New Modified EWMA Control Chart for Monitoring Processes Involving Autocorrelated Data. Intelligent Automation and Soft Computing, 36(1), 281–298. doi:10.32604/iasc.2023.032487.

[28] Silpakob, K., Areepong, Y., Sukparungsee, S., & Sunthornwat, R. (2023). Exact Average Run Length Evaluation for an ARMAX (p, q, r) Process Running on a Modified EWMA Control Chart. IAENG International Journal of Applied Mathematics, 53(1), 1-11.

[29] Peerajit, W. (2023). Developing Average Run Length for Monitoring Changes in the Mean on the Presence of Long Memory under Seasonal Fractionally Integrated MAX Model. Mathematics and Statistics, 11(1), 34–50. doi:10.13189/ms.2023.110105.

[30] Phanthuna, P., Areepong, Y., & Sukparungsee, S. (2021). Detection capability of the modified EWMA chart for the trend stationary AR (1) model. Thailand Statistician, 19(1), 69-80.

[31] Petcharat, K. (2022). The Effectiveness of CUSUM Control Chart for Trend Stationary Seasonal Autocorrelated Data. Thailand Statistician, 20(2), 475–488.

[32] Supharakonsakun, Y., & Areepong, Y. (2022). Design and Application of a Modified EWMA Control Chart for Monitoring Process Mean. Applied Science and Engineering Progress, 15(4), 5198. doi:10.14416/j.asep.2021.06.007.

[33] Karoon, K., Areepong, Y., & Sukparungsee, S. (2023). Trend Autoregressive Model Exact Run Length Evaluation on a Two-Sided Extended EWMA Chart. Computer Systems Science and Engineering, 44(2), 1143–1160. doi:10.32604/csse.2023.025420.

[34] Karoon, K., Areepong, Y., & Sukparungsee, S. (2023). On the Performance of the Extended EWMA Control Chart for Monitoring Process Mean Based on Autocorrelated Data. Applied Science and Engineering Progress, 16(4), 6599. doi:10.14416/j.asep.2023.01.004.

[35] Almousa, M. (2020). Adomian decomposition method with modified Bernstein polynomials for solving nonlinear Fredholm and volterra integral equations. Mathematics and Statistics, 8(3), 278–285. doi:10.13189/ms.2020.080305.

[36] Sofonea, M., Han, W., & Shillor, M. (2005). Analysis and approximation of contact problems with adhesion or damage. Chapman & Hall/CRC, New York, United States. doi:10.1201/9781420034837.

[37] Alevizakos, V., Chatterjee, K., & Koukouvinos, C. (2021). The triple exponentially weighted moving average control chart. Quality Technology and Quantitative Management, 18(3), 326–354. doi:10.1080/16843703.2020.1809063.